PRS GLOBAL OPEN

EXPERIMENTAL

Blood Supply to the Integument of the Abdomen of the Rat: A Surgical Perspective

Diogo Casal, MD*†‡§
Diogo Pais, MD, PhD†
Inês Iria, MSci§¶
Paula A. Videira, PhD‡§∥
Eduarda Mota-Silva, MSci**
Sara Alves, MSci††
Luís Mascarenhas-Lemos, MD††
Cláudia Pen, MSci††
Valentina Vassilenko, PhD**
João Goyri-O'Neill, MD, PhD†

Background: Many fundamental questions regarding the blood supply to the integument of the rat remain to be clarified, namely the degree of homology between rat and humans. The aim of this work was to characterize in detail the macro and microvascular blood supply to the integument covering the ventrolateral aspect of the abdominal wall of the rat.
Methods: Two hundred five Wistar male rats weighing 250–350 g were used. They were submitted to gross anatomical dissection after intravascular colored latex injection (n = 30); conversion in modified Spalteholz cleared specimens (n=10); intravascular injection of a Perspex solution, and then corroded, in order to produce vascular corrosion casts of the vessels in the region (n = 5); histological studies (n = 20); scanning electron microscopy of vascular corrosion casts (n = 10); surgical dissection of the superficial caudal epigastric vessels (n = 100); and to thermographic evaluation (n = 30).
Results: The ventrolateral abdominal wall presented a dominant superficial vascular system, which was composed mainly of branches from the superficial caudal epigastric artery and vein in the caudal half. The cranial half still received significant arterial contributions from the lateral thoracic artery in all cases and from large perforators coming from the intercostal arteries and from the deep cranial epigastric artery.
Conclusions: These data show that rats and humans present a great deal of homology regarding the blood supply to the ventrolateral aspect of the abdominal integument. However, there are also significant differences that must be taken into consideration when performing and interpreting experimental procedures in rats. (*Plast Reconstr Surg Glob Open 2017;5:e1454; doi: 10.1097/GOX.0000000000001454; Published online 11 September 2017.*)

INTRODUCTION

The rat is arguably the most commonly used animal model for training and research in plastic surgery.[1–11] Its abdominal wall is frequently employed in tissue perfusion

and transference studies.[12–18] Oddly, anatomical and histological studies concerning the blood supply to the integument over the ventrolateral aspect of the abdomen of the rat (IOVAAR) are scant and are based on small series of animals.[19] Hence, many fundamental questions remain to be clarified, namely the degree of homology between it and that of humans.[19] The aim of this work was to characterize in detail the macro and microvascular blood supply to the IOVAAR.

METHODS

This study focused on the blood supply to the IOVAAR, defined by the region ventral to the dorsal axillary lines. Two hundred five Wistar male rats weighing 250–350 g were used.

Supplemental digital content is available for this article. Clickable URL citations appear in the text.

All the animals were housed under standard environmental conditions and given nothing by mouth 6 hours before surgical procedures.

All in vivo studies were performed in strict accordance with the recommendations in the Guide for Proper Conduct of Animal Experiments and Related Activities in Academic Research and Technology, 2006.

The protocol was approved by the Institutional Animal Care and Use Committee and Ethical Committee at the authors' institution (08/2012/CEFCM).

Gross Anatomical Dissection

In 30 rats, a 22G catheter was introduced in the left ventricle and another in the right ventricle. A volume of 180–200 ml/kg of a red colored latex solution (Robialac) was introduced in the left ventricle and a volume of 300–350 ml/kg of a blue colored latex solution (Robialac) was introduced in the right ventricle, until good peripheral contrast perfusion was noted. Subsequently, the rats were submitted to abdominal wall dissection to characterize the origin of the supplying vessels. This technique allows to highlight the vessels as they are normally observed during surgical procedures.[20]

In 10 rats subjected to a similar procedure, the IOVAAR was converted into modified Spalteholz cleared specimens.[21] This technique creates transparent 3-dimensional specimens, while preserving vascular and perivascular structure.[22]

Five rats were submitted to a left ventricular injection of a Perspex solution, and then corroded, to produce vascular corrosion casts of the vessels in the IOVAAR. Vascular corrosion casts produce a faithful replica of vascular beds, allowing detailed 3-dimensional morphological analysis of even small vessels.[23]

All identified perforator vessels were plotted on a Cartesian grid centered on the pubic symphysis.

Microscopic Anatomical Study—Optical Microscopy

Ten rats were submitted to surgical collection of the IOVAAR, which was fixed in 10% paraformaldehyde and prepared for histological examination, using hematoxylin-eosin and Masson's trichrome stains, as well as immunohistochemistry for CD31 for staining the endothelium[24–26] and for neurofilaments for staining nerves.[27] Rats were submitted to axial sections in the caudal, middle, and cranial aspect of both sides of the abdomen. Ten additional rats were subjected to the preparation just described and their largest integumentary veins were sectioned longitudinally for evaluation of venous valves.

Microscopic Anatomical Study—Scanning Electron Microscopy of Vascular Corrosion Casts

Ten rats were submitted to intravascular injection of a resin cast (Mercox) and latter corroded.[28] The vascular casts were processed and examined using 2 scanning electron microscopes (acceleration voltage of 2–30 kV): a JEOL JSM-5410, for histomorphometric analysis, and a JEOL JSM-7001F, for obtaining high-quality images. Vascular casts were interpreted according to Aharinejad and Lametschwandtner.[28]

Surgical Anatomy of the Superficial Caudal Epigastric Vessels

In 100 rats used for surgical training and experiments, the origin of the superficial caudal epigastric vessels (SCEVs) was registered on the left side of the abdomen.

The specimens were photographed using adequate microscopes. Vessels' dimensions were determined using the ImageJ software.

Thermographic Evaluation

In 30 rats, thermographic assessment of the IOVAAR was performed with a FLIR E6 camera placed 25 cm above the abdomen. Evaluations were done after the rats were anesthetized intraperitoneally with a mixture of ketamine and diazepam and placed on their backs for 10 minutes. The day before the evaluation, animals were lightly anesthetized and the hair of the abdominal area removed using a depilatory cream. Evaluations were performed at a constant room temperature (22°C) and humidity (50%).[29]

Statistical Analysis

Qualitative variables were expressed as percentages. Quantitative variables were expressed as means ± SD. The SPSS 21.0 software was used for statistical analysis. The Kolmogorov-Smirnov test was used to assess normality. Analysis of variance and Student's t test were used to compare averages in normally distributed data. Kruskal-Wallis and Mann-Whitney tests were used to compare means in nonnormally distributed data. Proportions were analyzed with the chi-square test or Fisher's exact test.

A cluster analysis was performed using a 2-step clustering procedure based on the Schwarz Bayesian criteria to determine the overall distribution of all significant cutaneous perforators.

A 2-tailed $P < 0.05$ was considered to be statistically significant.

RESULTS

Gross Anatomy

Figure 1 summarizes the most common disposition found in the main vessels supplying the IOVAAR. This region presented a dominant superficial vascular system (Figs. 2–4; **see figure, Supplementary Digital Content 1**, which demonstrates lateral thoracic (LT) vessels and their anatomical relations, *http://links.lww.com/PRSGO/A503*). In the caudal half, this system was composed mainly of branches from the superficial caudal epigastric artery (SIEA) and vein (SIEV), which are the equivalent to the human superficial inferior epigastric artery and vein. The cranial half also received significant arterial contributions from the LT artery in all cases, and from 1 (64.4%), 2 (26.7%), or 3 (8.9%) large perforators coming from the intercostal arteries, and from the deep cranial epigastric artery, forming, in this latter case, the superficial cranial epigastric artery (present in 95.6%
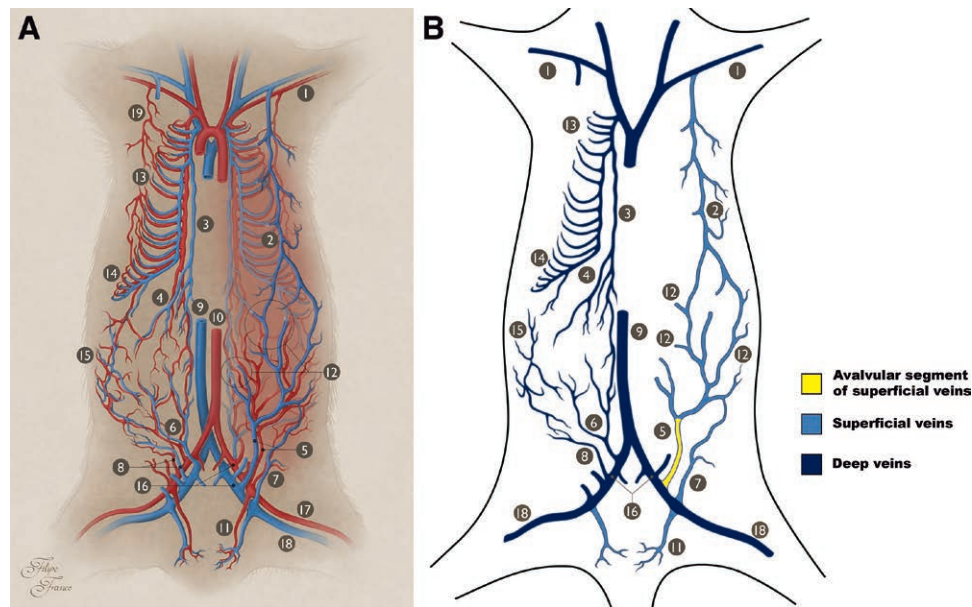
Fig. 1. Macrovascular blood supply to the IOVAAR. A, Schematic drawing illustrating the major vessels supplying IOVAAR. On the right side of the picture, the superficial vessels (superficial to the muscle fascia) are represented in full. On this side, the deeper vessels (deep to the muscle fascia) are represented in a lighter color. On the left side of the picture, only the deeper vessels (deep to the muscle fascia) are represented. Blue structures represent veins. Red structures represent arteries. B, Schematic drawing illustrating the major veins draining the IOVAAR, as represented in 1A. On the left side of the picture are represented the deep veins (deep to the muscle fascia), whereas on the right side of the picture are represented the superficial veins. The valvular and avalvular segments are shown. 1, Axillary artery and vein; 2, LT (thoracoepigastric) vein; 3, internal thoracic artery and vein; 4, cranial epigastric artery and vein; 5, SIEA and vein; 6, deep caudal epigastric artery and vein; 7, superficial circumflex iliac artery and vein; 8, deep circumflex iliac artery and vein; 9, caudal vena cava; 10, abdominal aorta; 11, superficial EPA and vein; 12, perforator arteries and veins; 13, cranial intercostal arteries and veins; 14, caudal intercostal arteries and veins; 15, lumbar (or iliolumbar) arteries and veins; 16, external iliac artery and vein; 17, femoral artery; 18, femoral vein; 19, LT artery.

of cases on the right side and 93.3% of cases on the left side). Most of the lateral and cranial aspects of the IOVAAR drained into the tributaries of the large LT vein (thoracoepigastric vein). In all cases, the lateral branch of the SIEV and the branches that originated the LT vein were anastomosed in the lateral aspect of the midportion of the abdomen (Figs. 3, 4).

The IOVAAR received relatively minor contributions from the comparatively diminutive deep inferior epigastric system, from the terminal branches of the last 6 intercostal vessels and lumbar/iliolumbar vessels, from the thoracodorsal vessels, from the deep and superficial circumflex iliac vessels, and from the external pudendal vessels.

The Angiosomes of the IOVAAR

The angiosomes of the IOVAAR are represented in Figure 2. The SCEVs presented numerous variations (**see figure, Supplementary Digital Content 2**, which demonstrates schematic representation of the variations in the origin, termination, and distribution of the SIEA and vein, respectively, and the external pudendal artery (EPA) and vein on the left side of the rat, ***http://links.lww. com/PRSGO/A504***). The frequency of each variation is shown at the top right hand corner of each drawing. The

total number of rats analyzed was 185 (http://links.lww. com/PRSGO/A504). In most cases (71.7%), the SIEA and the EPA originated from a common trunk called pudendoepigastric arterial trunk. In only 28.3% of cases did the SIEA and the superficial EPA arise as isolated vessels. The SIEA and the EPA were each accompanied by a comitant vein that had a parallel course, draining either into the pudendoepigastric venous trunk or into the femoral vein.

After its origin, the SIEA moved obliquely in the direction of the axilla. In all cases, this artery divided into 2 branches, being followed in its trajectory toward the axilla by its lateral branch. The lateral branch of the SIEA was larger than its medial counterpart in nearly all cases (94.5% of cases on the right side and 95.6% on the left side). The lateral branch anastomosed with the terminal branches of the LT artery and with the dominant perforators originating from the intercostal vessels. The medial branch of the SIEA anastomosed with the superficial cranial epigastric artery and/or with perforators of the deep cranial epigastric artery (Figs. 2–4; **Supplementary Digital Content 1**, ***http://links.lww.com/ PRSGO/A503***).

The large LT vein could be found in a line drawn from the rat's hip to the ipsilateral axilla (Figs. 3, 4; **Supple-**
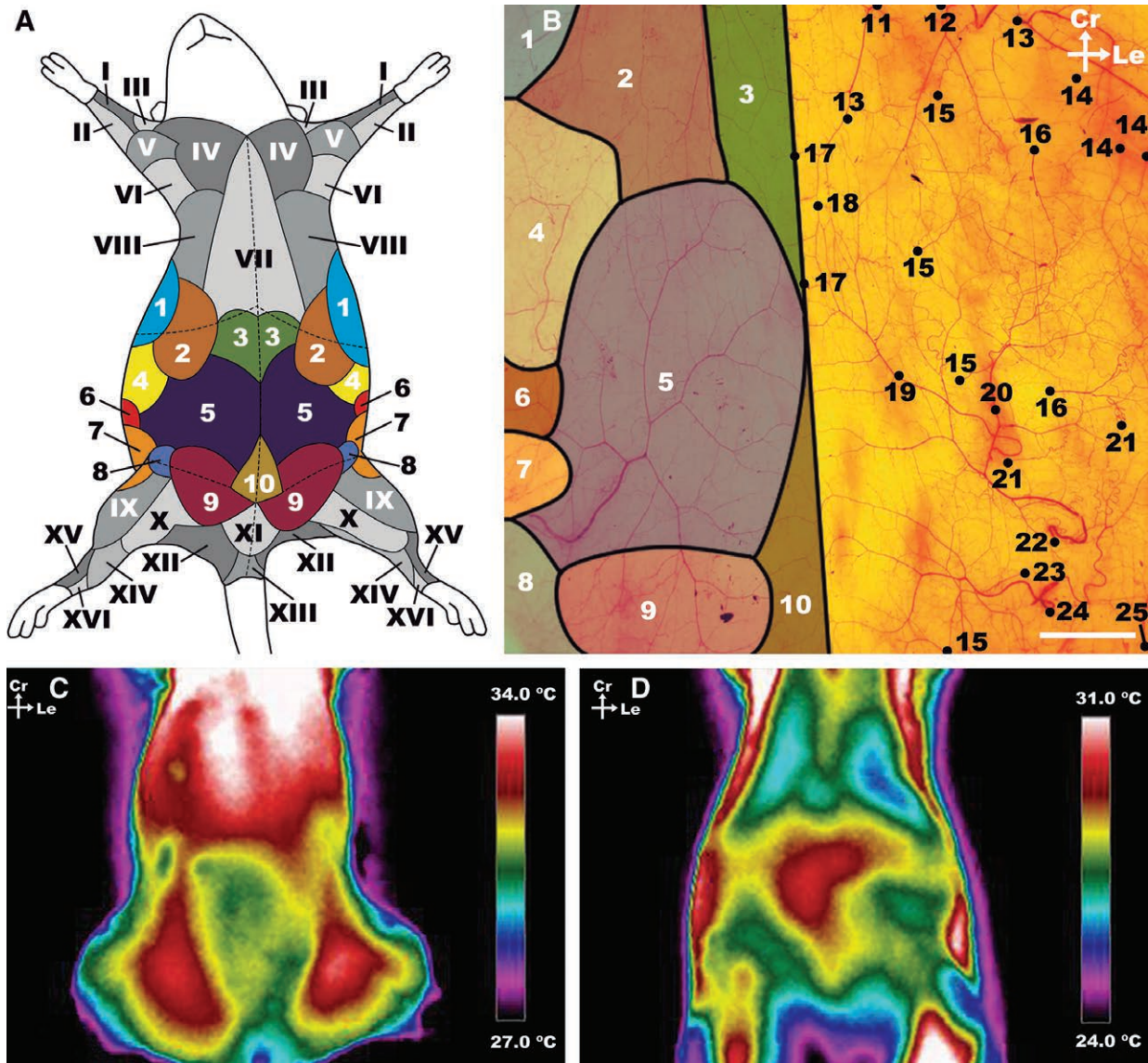
Fig. 2. Macrovascular blood supply to the ventrolateral aspect of the rat's abdominal wall. A, Schematic representation of the angiosomes of the ventrolateral aspect of the rat. The angiosomes of the abdomen studied in the present study are represented are numbered in Arabic numerals and represented in different colors. The adjacent angiosomes are numbered in roman numerals and highlighted in different levels of gray. These angiosomes have been represented according to Taylor et al.[32,33] and Kochi et al.[40] B, Photograph of the integument covering the ventrolateral aspect of the abdomen of the rat after processing by the modified Spalteholz technique showing the supplying vessels and respective angiosomes. The top limit of the photograph corresponds to the lower limit of the rib cage, the lower limit to a transverse line abutting the pubic symphysis; the lateral limits of the photograph correspond to the dorsal axillary lines. C and D, Representative infrared thermography images of the ventrolateral aspect of the abdomen of the rat. C, Direct infrared thermography with hotspots in the region of the dominant axial vessels (the caudal superficial epigastric vessels). D, Infrared thermography after cooling of the rat's surface, by placing a silicone gel bag at a temperature of approximately 21ºC for 2 minutes. This image shows the location of the dominant perforator vessels in the central and cranial aspect of the abdomen. The thermograms were taken for a period of 5 minutes with 30-second intervals. Ca, caudal; Cr, cranial; Le, left; La, lateral; M, medial. I, median angiosome; II, ulnar angiosome; III, deep brachial angiosome; IV, transverse cervical angiosome; V, dorsal circumflex humeral angiosome; VI, circumflex scapular angiosome; VII, internal thoracic angiosome; VIII, cranial intercostal perforators angiosome; IX, lateral circumflex femoral angiosome; X, medial circumflex femoral angiosome; XI, superficial external pudendal angiosome; XII, caudal gluteal angiosome; XIII, internal pudendal angiosome; XIV, saphenous angiosome; XV, fibular angiosome; XVI, anterior tibial angiosome. 1, thoracodorsal angiosome; 2, LT angiosome; 3, cranial epigastric angiosome; 4, caudal intercostal perforators angiosome; 5, superficial caudal epigastric angiosome; 6, lumbar (or iliolumbar) perforators angiosome; 7, deep circumflex iliac angiosome; 8, deep external pudendal angiosome; 9, superficial external pudendal angiosome; 10, deep caudal epigastric angiosome; 11, cranial deep epigastric artery perforator; 12, LT artery; 13, thoracodorsal artery perforator; 14, intercostal perforators; 15, perforators from the medial branch of the deep caudal and cranial epigastric arteries; 16, perforators from the lateral branch of the deep caudal and cranial epigastric arteries; 17, choke vessels between the two superficial caudal epigastric angiosomes; 18, anastomoses between the superficial caudal epigastric arteries and the LT arteries; 19, medial branch of the SIEA; 20, lateral branch of the SIEA; 21, lumbar perforators; 22, SIEA; 23, superficial EPA; 24, deep EPA; 25, deep circumflex iliac artery. Calibration bar = 10 mm.
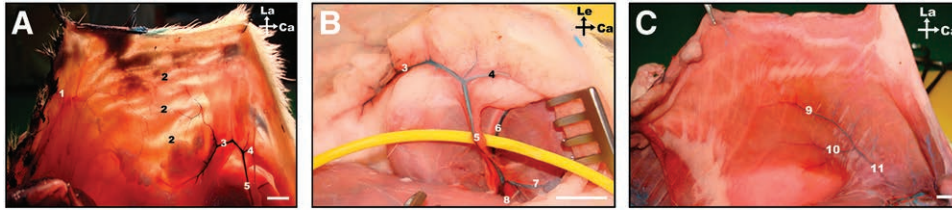
Fig. 3. Macrovascular blood supply to the ventrolateral aspect of the rat's abdominal wall. A, Photograph under transillumination of the integument covering the left side of the abdomen showing its largest vessels. B, Photograph of the left groin region showing the origin of the SCEVs from the femoral vessels; C, Photograph of the deep surface of the left rectus abdominis muscle, showing the deep caudal epigastric vessels supplying this muscle; Ca, caudal; Cr, cranial; Le, left; La, lateral; M, medial. 1, LT artery; 2, anastomoses between the superficial caudal epigastric arteries and the LT arteries; 3, lateral branch of the SIEA; 4, medial branch of the SIEA; 5, SIEA; 6, femoral vessels and nerve; 7, Deep EPA; 8, superficial EPA; 9, medial branch of the deep caudal epigastric artery; 10, lateral branch of the deep caudal epigastric artery; 11, deep caudal epigastric vessels; 12, cranial deep epigastric artery perforator; 13, xyphoid process; 14, perforators from the medial branch of the deep caudal and cranial epigastric arteries; 15, intercostal perforators; 16, lumbar perforators. Calibration bar = 10 mm.
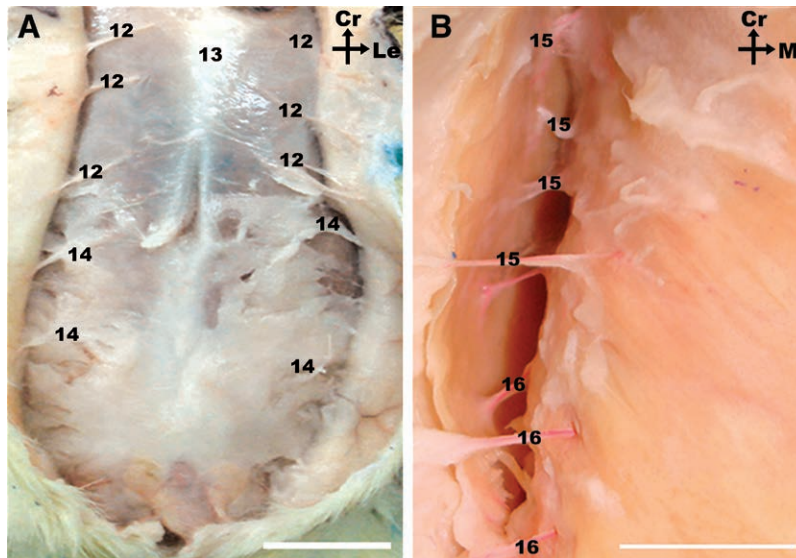

Fig. 4. A, Photograph of the integument of the ventral region of the abdomen of the rat, after midline incision and partial lateral retraction, showing multiple perforators supplying this region coming off the deep cranial and caudal epigastric vessels. B, Photograph of the right flank of the abdomen showing multiple lateral perforators supplying the lateral aspect of the integument of the rat in this region Calibration bar = 10 mm.

mentary Digital Content 1, *http://links.lww.com/PRSGO/A503*). This vein originated at the level of the costal margin from the convergence of 3 veins that drained the medial, central, and lateral portion of the cranial aspect of the IOVAAR.

The SIEA and the SIEV were accompanied by a sizeable branch of the saphenous nerve—the caudal epigastric nerve (Fig. 5). At its origin, the diameter of this nerve was 0.33±0.17 mm. It divided into 2, 3, or 4 branches in the proximal third of the SIEA in 60.6%, 13.1%, and 26.2% of cases, respectively. These branches traveled with the SIEA from its origin and in turn provided multiple twigs throughout the territory of the SCEVs and also to the medial aspect of the thigh.

Musculocutaneous Perforators

Multiple sizeable perforator vessels were seen piercing the muscles and muscular fascia and supplying the IOVAAR (Figs. 2–4, 6; **Supplementary Digital Content 1**, *http://links.lww.com/PRSGO/A503*). These perforators were most commonly seen arising from the rectus abdominis fascia in the central aspect of the abdomen (Fig. 7). In this region, the superficial vascular system was less dense (Fig. 2). The largest central abdominal perforators derived mainly from the deep epigastric vessels and particularly from the cranial deep epigastric vessels. On each side, there were on average 6.52±3.64 perforators on the right side and 6.56±3.67 perforators on the left side, ranging between 2 and 15.
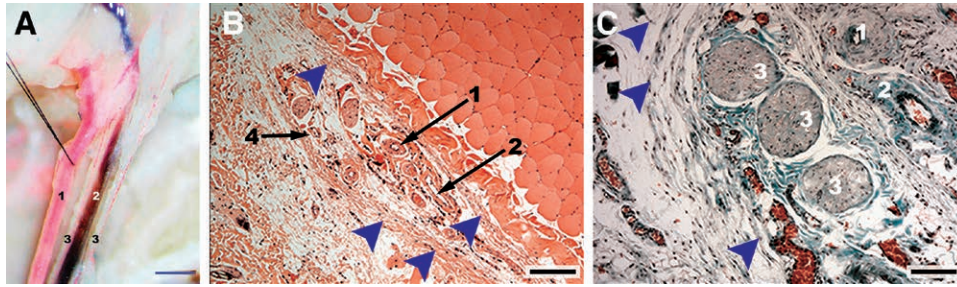
Fig. 5. Superficial caudal epigastric neurovascular bundle and its branches. A, Photograph of the superficial caudal epigastric neurovascular bundle after intraarterial and intravenous injection with a red and blue solution, respectively. B, Microphotograph of a hematoxylin-eosin–stained section of a transverse section of the caudal superficial epigastric neurovascular bundle. C, Microphotograph of a Masson's trichrome stained section of a transverse section of the caudal superficial epigastric neurovascular bundle. 1, SIEA; 2, superficial caudal epigastric vein; 3, branches of the caudal epigastric nerve; 4, superficial caudal epigastric lymphatic vessels. Arrow heads indicate the sheath involving the superficial caudal epigastric neurovascular bundle. Calibration bar in A = 1000 μm; calibration bars in B and C = 100 μm.

Overall, 79.1% of perforators originated in the deep epigastric system, whereas 28.1% originated in the segmental vessels that supplied the abdominal wall (last 6 intercostal, lumbar/iliolumbar, and the deep circumflex iliac vessels). This difference was statistically significant ($P < 0.05$). Perforators were more common in the cranial half of the abdomen, that is to say in the region were the axial vessels were inexistent or of a smaller caliber [$P < 0.05$; Fig. 7; **see figure, Supplementary Digital Content 3**, which demonstrates a dot plot graph drawn over a schematic drawing of the ventrolateral surface of the rat showing the location of the abdominal perforator arteries in the anterior and lateral aspect of the abdominal wall and their origin from the paramedian arteries (cranial and caudal deep epigastric arteries) and from the segmental vessels (intercostal, lumbar/iliolumbar arteries), *http://links.lww.com/PRSGO/A505*]. A 2-step cluster analysis based on the Schwarz Bayesian criteria allowed the identification of 7 musculocutaneous perforator clusters on each side of the abdomen (Fig. 7).

Table 1 summarizes the main histomorphometric features of the largest vessels supplying the IOVAAR. No statistically significant differences were found between the right and left sides of the body.

Noteworthy is the large direct cutaneous vessels described above were present in areas where the integument was laxer, whereas the musculocutaneous perforators were placed more densely in the region where the IOVAAR was more adherent to the underlying muscle fascia. Moreover, the perforator vessels were longer in the lateral aspect of the abdomen compared with those that were more centrally placed in the region of the rectus abdominis muscles. Interestingly, on each side of the abdomen, there was a triangular region, lateral to the lateral branch of the SCEVs, where large vessels were absent (**see figure, Supplementary Digital Content** 4, which demonstrates a schematic diagram illustrating the safe zones (blue) for subcutaneous and intraperitoneal injections in the ventrolateral abdomen of the rat due to the relative scarcity of large vessels in these areas, *http://links.lww.com/PRSGO/A506*).

Microscopic Anatomy

The IOVAAR was composed of multiple layers, including a sheath of loose connective tissue associated with white adipose tissue and smooth muscle known as panniculus carnosus (Fig. 6; **see figure, Supplementary Digital Content 5**, which displays a general view of the blood supply to the different layers of the ventrolateral aspect of the abdominal wall of the Wistar rat, *http://links.lww.com/PRSGO/A507*). Soon after their origin, the large nominated vessels with an axial pattern were found in the panniculus adiposus, immediately superficial to the panniculus carnosus layer. These vessels gave ascending branches to all layers of the IOVAAR, including the panniculus carnosus. The musculocutaneous perforator vessels originated arterioles and received venules to and from the muscular subfascial, fascial, and epifascial plexuses. Additionally, in their ascending trajectory toward the skin, they gave branches to all the layers of the IOVAAR. Overall, integumentary vessels formed fine interconnecting meshworks of predominantly horizontal arrangement, establishing the following vascular plexuses: prefascial plexus, panniculus carnosus plexus, panniculus adiposus plexus, subdermal plexus, reticular dermal plexus, and subpappilary dermal plexus (Figs. 3–7; Supplementary Digital Content 1, 5, 6; **see figure, Supplementary Digital Content 6**, which shows details of the blood supply to the different layers of the ventrolateral aspect of the abdominal wall of the Wistar rat, *http://links.lww.com/PRSGO/A508*).

At the subdermal and the subpapillary vascular plexuses, scattered and rare arteriovenous anastomoses were found. Precapillary sphincters were frequent findings at the subdermal and reticular dermis plexuses. Multiple venous valves were found in all layers of the integument, from the reticular dermis plexus until the major nominated veins. However, the first-order subdermal veins presented large segments devoid of valves. Venous valves were almost always bicuspid, although a few tricuspid valves were observed. All the nominated veins and their tributaries presented venous valves, with the exception of the SIEV itself, which presented no valves in all specimens studied (**see figure, Supplementary Digital Content**
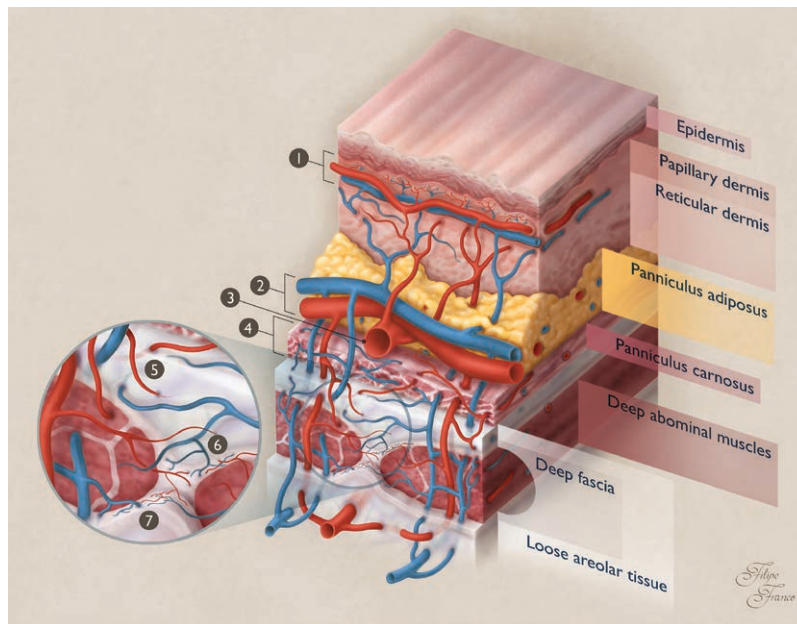
Fig. 6. Schematic drawing of the blood supply to the different layers of the integument of the ventrolateral aspect of the abdomen of the rat. The integument of the rat is composed of the skin, a fatty layer known as panniculus adiposus, and beneath this latter layer of a sheath of loose connective tissue associated with white adipose tissue and smooth muscle forming a layer known as panniculus carnosus. This layer is located just above the abdominal wall muscles and muscle fascias. There is a loose areolar tissue beneath the panniculus carnosus and the muscle fascia. The integument presented the following plexuses: a loose and thin prefascial plexus in the prefascial areolar tissue; a dense and thin panniculus carnosus plexus encompassing the entire thickness of this layer and mostly dependent on the direct cutaneous axial vessels. This plexus was mostly composed of third-order arterioles and venules, as well as capillaries; a loose panniculus adiposus plexus, mainly composed of obliquely disposed ascending and descending first-order arterioles and venules, respectively, supplying the overlying layers and the adjacent fatty tissue; a subdermal plexus at the upper portion of the panniculus adiposus, immediately beneath the skin, composed of second-order arterioles and venules with a horizontal orientation; a reticular dermal plexus composed of vertically arranged third-order ascending and descending arterioles and venules, respectively, as well as their terminal branches, which formed capillary networks around sebaceous dermal glands and the papillae of hair follicles; a subpappilary dermal plexus, at the dermal-epidermal interface, composed of capillary loops with a predominantly horizontal disposition interspersed with occasional vertical capillary loops. These capillaries were in continuity with the vertical arterioles and venules of the reticular plexus. Blue structures represent veins. Red structures represent arteries. 1, Subpapillary vascular plexus; 2, subdermal vascular plexus; 3, superficial arteriole in the panniculus adiposus; 4, panniculus carnosus vascular plexus; 5, arterioles and venules supplying the prefascial vascular plexus in the prefascial areolar tissue; 6, fascial vascular plexus; 7, subfascial vascular plexus.

7, which demonstrates a venous drainage of the integument of the ventrolateral abdomen of the rat, *http://links. lww.com/PRSGO/A509*; **see figure, Supplementary Digital Content 8**, which demonstrates details of the microvascular blood supply to the integument covering the ventrolateral aspect of the abdomen of the rat, *http://links.lww. com/PRSGO/A510*).

Each of the branches of the caudal epigastric nerve presented a monofascicular pattern (Fig. 5). The average number of nerve fibers in the proximal portion of this nerve was 1093.00 ± 88.32 on the right side and 1051.50 ± 107.39 on the left side, being overall 1072.20 ± 97.80. The difference between sides was not statistically significant.

Thermographic Results

Figure 2 illustrates the typical infra-red thermographic images of the IOVAAR obtained directly and post cooling of the rat's surface. In all cases, direct thermography showed a region of higher temperature corresponding to the territory of the SCEVs and the LT vessels. Post cooling thermography, used to highlight perforator vessels, showed a region of higher temperatures in the central and cranial aspect of the abdomen.

DISCUSSION

The IOVAAR has been used regularly for training and research purposes since at least 1967 when the rat

epigastric flap was described.[30] Surprisingly, few studies have addressed the macroscopic vascular anatomy of this region.[4,7,31–37] Furthermore, the literature on the microvascular blood supply to the rat's integument is even scarcer, being restricted to the paw and tail regions.[28,38] As far as the authors could determine, the present series, comprising 205 rats, is the largest on the macroscopic and

microscopic anatomy of the vascular blood supply to the IOVAAR.

Numerous doubts persist regarding the extent of similarity between the blood supply to this region in humans and rats. Some authors state that the blood supply is relatively similar,[31] whereas others argue that it is substantially different.[32] Table 2 summarizes the main differences found in the present study. Overall, although there are some strong analogies between rats and the humans, namely a common vascular framework (Figs. 1, 6), there are also some noteworthy differences.

The most striking difference refers to the preponderance of the direct cutaneous vessels in the rat, compared with the dominance of the musculocutaneous vessels in humans. Taylor[32,33] attributed this difference to the fact that in loose-skinned animals, like the rat, the integument is more mobile relative to the underlying muscles due to the presence of a loose areolar tissue layer between the muscular fascia and the panniculus carnosus (Fig. 6). The corollary of this is a greater dependence on direct cutaneous vessels in loose-skinned animals compared with humans.[32,33] Interestingly, in the present study, the greater number of perforators was in fact found close to the midline, an in particular in the cranial half of the abdomen, precisely where the integument of the rat was more adherent to the underlying muscle fascia (Fig. 7). In this region, the superficial vascular system was less dense (Fig. 1).

Another important difference found in this work relative to humans is that central abdominal perforators in the rat were derived mostly from the deep cranial epigastric artery and not from the deep inferior epigastric vessels as in the former species.[34] These findings are supported by the 2 other articles that systematically evaluated the number and location of musculocutaneous perforators of the rat's abdomen.[34,37] Hence, perforator flaps in the IOVAAR seem to be substantially different from those in humans, in terms of vascular homology.

An additional difference relative to humans is the importance of the vessels in the panniculus carnosus of the rat for integumentary perfusion. This had already been hinted by the greater survival of flaps that included this layer, comparatively to flaps that excluded it.[39] In fact, we observed that, soon after their origin, the major subcutaneous vessels coursed in the panniculus adiposus immedi-
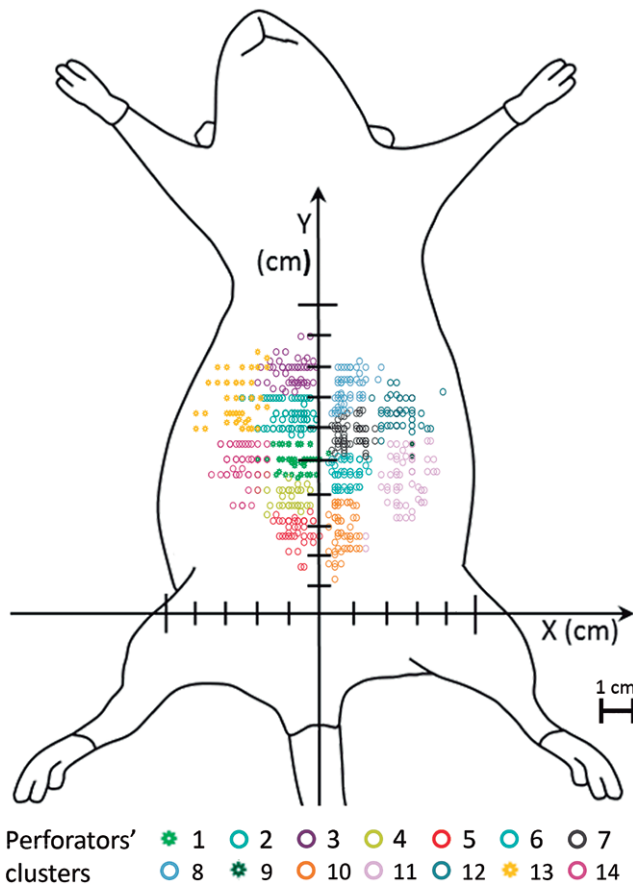

Fig. 7. Dot plot graph drawn over a schematic drawing of the ventrolateral surface of the rat showing the location of the abdominal perforator arteries in the anterior and lateral aspect of the abdominal wall. A two-step cluster analysis based on the Schwarz Bayesian criteria allowed the identification of 7 perforator clusters on each side of the abdomen.

Table 1. Histomorphometric Evaluation of the Major Arteries and Veins Supplying the Ventrolateral Region of the Integument of the Abdomen of the Rat

Vessel	Length* (cm)	Caliber† (mm)	Wall Thickness‡ (µm)
SIEA	1.45±0.22	0.32±0.13	479.07±27.37
SCEV	1.61±0.19	0.65±0.24	183.05±15.63
First divisions of the SIEA	0.72±0.16	0.13±0.08	288.19±31.72
First divisions of the SCEV	0.92±0.18	0.18±0.05	128.24±43.53
Second divisions of the SIEA	0.60±0.12	0.08±0.03	202.38±87.34
Second divisions of the SCEV	0.85±0.20	0.16±0.09	102.63±65.71
Thoracoepigastric vein	4.13±1.59	0.47±0.17	41.67±15.67
First divisions of the thoracoepigastric vein	1.63±0.47	0.17±0.04	0.11±0.09
Second divisions of the thoracoepigastric vein	0.96±0.54	0.14±0.05	0.09±0.08

Values are expressed as average values ± SD.
*Length determination was based on Spalteholz cleared specimens (n = 10).
†Caliber determination was based on Spalteholz cleared specimens (n = 10), on transverse histological sections stained with CD 31 (n = 10) and on the scanning electron microscopy observation of the vascular corrosion casts (n = 10).
‡Wall thickness determination was based on transverse histological sections stained with Masson's Trichrome (n = 10).

Table 2. Main Differences between the Usual Blood Supply to the Integument of the Ventrolateral Aspect of the Abdomen of Humans[33,57] and Rats

Anatomical Structure(s)	Humans	Rat
Dominant arteries	Musculocutaneous (in particular the deep inferior epigastric artery)	Direct cutaneous (in particular the SIEA/superficial inferior epigastric artery)
Dominant veins	Superficial and deep veins (in particular the deep inferior epigastric veins and the superficial inferior epigastric vein)	Superficial veins (in particular the LT vein/thoracoe-pigastric vein and the SCEV/superficial inferior epigastric vein)
SIEV	Frequently absent or hypoplasic	Always present and with a sizeable caliber
Perforator vessels	Major role in the normal perfusion; more numerous; more abundant laterally and below the umbilicus	Less important role in integumentary perfusion; less numerous; mostly located in an area cranially to the umbilicus
Venous valves	Uniformly present in the superficial and deep venous systems	More abundant in the deep venous system and in the cranial aspect of the superficial venous system
Panniculus carnosus	Absent	Well-developed and associated with a vascular plexus
Nerves accompanying major vessels	Intercostal nerves 7–12 accompanying the homonymous vessels	Intercostal nerves 7–12 accompanying the homony-mous vessels; caudal epigastric nerve/inferior epigastric nerve is a sizeable and constant nerve that is part of the superficial caudal epigastric neurovas-cular bundle

Fig. 8. Vascular pedicle of common flaps raised on the ventrolateral surface of the abdomen of the rat. Some of the most common flaps performed in this region are the TRAM flap based on the cranial epigastric vessels; the SCIA flap (also known as iliofemoral flap) based on the superficial circumflex iliac vessels; the DIEP flap based on the perforator vessels originating from the deep cranial epigastric vessels; the DSCI flap (also known as iliac osteocutaneous flap) based on the deep circumflex iliac vessels; the SIEA flap (also known as groin flap) based on the SCEVs; the EOMA perforator flap based on the perforators originating from the 6 last intercostal vessels or from the lumbar vessels; and the VRAM flap. 1, TRAM flap based on the cranial epigastric vessels; 2, SCIA or iliofemoral flap based on the superficial circumflex iliac vessels; 3, DIEP flap based on the perforator vessels originating from the deep cranial epigastric vessels; 4, DSCI or iliac osteocutaneous flap based on the deep circumflex iliac vessels; 5, SIEA or groin flap based on the SCEVs; 6, EOMA perforator flap based on the perforators originating from the last 6 caudal intercostal vessels or from the ilolumbar vessels; 7, VRAM flap. DIEP, deep inferior epigas-tric artery perforator; DSCI, deep circumflex iliac artery; EOMA, external oblique myocutaneous artery; SCIA, superficial circumflex iliac artery; TRAM, transverse rectus abdominis myocutaneous; VRAM, verti-cal rectus abdominis myocutaneous.

ately superficial to panniculus carnosus. In addition, the panniculus carnosus was provided with a vascular plexus of its own that was connected with the deep vascular system through anastomoses with branches of the musculocutane-ous perforators (Fig. 6; **see Supplementary Digital Content 5,** *http://links.lww.com/PRSGO/A507*, and **Supplementary Digital Content 6,** *http://links.lww.com/PRSGO/A508*).

Interestingly, the SCEVs in the rat presented nu-merous anatomical variations (**Supplementary Digi-**

tal Content 2, *http://links.lww.com/PRSGO/A504*). This had already been demonstrated in mice and hu-mans.[40–42]

Our data showed that in nearly all cases, the lateral branch of the SIEA was dominant relative to its medial counterpart. This is in accordance with the observations of Petry and Wertham[4] who suggested that part of the sur-vival variance of the rat epigastric flap could be explained by the inconsistent incorporation of this branch.

9

To the best of the authors' knowledge, the fascial envelope surrounding the superficial caudal epigastric neurovascular bundle and determining a specific compartment had not been described before. Notwithstanding, it is well known that when dissecting the superficial caudal epigastric pedicle, one has to tease away or to cut a delicate tissue sleeve that surrounds these structures. The superficial caudal epigastric fascia resembles the saphenous fascia that surrounds the saphenous veins in the lower limbs.[43] Acknowledging this fascial envelope may facilitate dissection of flaps in this region, particularly by novices in microsurgery.

An interesting information provided by this study was the identification of a triangular zone on each side of the IOVAAR where large vessels were absent (**Supplementary Digital Content 4**, *http://links.lww.com/PRSGO/A506*). These zones are probably safer for performing abdominal injections. As far as the authors could determine, these safe zones had not been described before.

Our thermographic analysis suggested that the most important perforators physiologically were located in the central and cranial aspect of the abdomen (Fig. 2). This information concurred with the anatomical dissection studies performed in the present studies and with those described by other authors.[34,35] Moreover, our thermographic examination also favored the notion that in normal conditions the superficial vessels were more important for supplying blood to the integument in the caudal and lateral aspects of the IOVAAR, whereas the perforator vessels were more important in the central and cranial aspects. Additionally, these data lend support to the use of thermography as a good technique for evaluating the most important perforator vessels in rats, as it had already been shown in humans by other authors.[29]

The presence of valves in the veins of the IOVAAR has been a matter of debate.[19] Our data show that multiple venous valves are found in all layers of the integument, from the reticular dermis plexus until the major nominated veins (**Supplementary Digital Content 5**, *http://links.lww.com/PRSGO/A507*, **Supplementary Digital Content 6**, *http://links.lww.com/PRSGO/A508*, **Supplementary Digital Content 7**, *http://links.lww.com/PRSGO/A509*, **Supplementary Digital Content 8**, *http://links.lww.com/PRSGO/A510*). However, the subdermal first-order venules presented large segments devoid of valves, which probably facilitate oscillating or bidirectional blood flow.[44] All the nominated veins and their tributaries presented venous valves, with the exception of the SIEV (Fig. 1B). Valdatta et al.[19] also failed to observe valves inside this vein. Scanning electron microscopy of vascular corrosion casts of human tissues revealed valves in superficial veins as small as 20 µm in diameter in different regions of the integument, and in particular in the lower limb, the anterior and posterior walls of the trunk.[45] The major difference between humans and rats regarding venous valves in these regions is, thus, the relative paucity of venous valves in the caudal aspect of the dominant venous system of rats, namely in the SIEV. This difference should be born in mind, for example, when using rats in experimental studies of tissue perfusion, namely in unconventional perfusion flaps and in particular in arterialized venous flaps.[46,47]

Human microcirculatory studies have shown that the skin subpapillary plexus presents an abundance of vertically arranged capillary loops, coinciding with the dermal papillae. These loops are more pronounced and numerous in body regions were the skin is thicker and subject to intense forces, namely in weight-bearing regions or the palm of the hands.[48] However, in our study and contrarily to what has been described in the skin in the footpad of the rat,[48,49] vertical capillary loops in the subpapillary plexus were relatively scarce. Capillaries were more frequently disposed in a horizontal manner in this region. These findings may be due to the fact that this region of the skin of the rat is thinner, has fewer dermal papillae, and it is not usually submitted to intense vertical forces (see **Supplementary Digital Content 5**, *http://links.lww.com/PRSGO/A507*, and **Supplementary Digital Content 6**, *http://links.lww.com/PRSGO/A508*).

In concordance with other microcirculatory studies performed in the skin covering the abdomen of humans, the authors found that there were few arteriovenous anastomoses in the IOVAAR.[48,50] This suggests that this region probably does not play a primordial role in thermoregulation.[50]

This study also lends support to the use of the epigastric flap as sensate flap, as proposed by Hirigoyen et al.[51] (Fig. 5). This construction has a similar anatomical rationale to that of using the 12th intercostal nerve in the human species to tailor a neurosensible fasciocutaneous SIEA flap.[51] However, a major difference between rats and humans is that in the former the SIEA and the caudal epigastric nerve are proportionally larger and are always present. Additionally, it should be noted that there is no exact human equivalent to the caudal epigastric nerve.[51]

One of the main limitations of the present work is that the histomorphometric data presented probably underestimate vessels' size, because optical microscopy images, as well as scanning electron microscopy images are known to be associated with vessels' shrinking during processing, resulting in underestimation of vessels' size of up to 30%.[28,52]

Finally, we believe that the anatomical study herein described helps to better plan, execute, and interpret the evolution of the multiple flaps performed in the IOVAAR for teaching, training, and research purposes (Fig. 8; **see pdf, Supplementary Digital Content 9**, which displays photographs illustrating the surgical anatomy of a few common flaps made on the ventrolateral aspect of the abdomen of the rat based on nominated vessels, *http://links.lww.com/PRSGO/A511*).[2,7,30,31,35,53–56]

CONCLUSIONS

The data presented in this article show that rats and humans present a great deal of homology regarding the blood supply to the ventrolateral aspect of the abdominal integument. However, there are also significant differences that must be taken into consideration when performing and interpreting experimental procedures in rats.

Diogo Casal, MD
Anatomy Department
NOVA Medical School
Universidade NOVA de Lisboa
Campo dos Mártires da Pátria, 130
1169-056, Lisbon
Portugal
E-mail: diogo_bogalhao@yahoo.co.uk

REFERENCES

1. Miles DA, Crosby NL, Clapson JB. The role of the venous system in the abdominal flap of the rat. *Plast Reconstr Surg*. 1997;99:2030–2033.
2. Okşar HS, Coşkunfirat OK, Ozgentaş HE. Perforator-based flap in rats: a new experimental model. *Plast Reconstr Surg*. 2001;108:125–131.
3. Ozgentaş HE, Shenaq S, Spira M. Development of a TRAM flap model in the rat and study of vascular dominance. *Plast Reconstr Surg*. 1994;94:1012–7; 1025.
4. Petry JJ, Wortham KA. The anatomy of the epigastric flap in the experimental rat. *Plast Reconstr Surg*. 1984;74:410–413.
5. Roberts AP, Cohen JI, Cook TA. The rat ventral island flap: a comparison of the effects of reduction in arterial inflow and venous outflow. *Plast Reconstr Surg*. 1996;97:610–615.
6. Sano K, Hallock GG, Rice DC. The relative importance of the deep and superficial vascular systems for delay of the transverse rectus abdominis musculocutaneous flap as demonstrated in a rat model. *Plast Reconstr Surg*. 2002;109:1052–7; discussion 1058.
7. Strauch B, Murray DE. Transfer of composite graft with immediate suture anastomosis of its vascular pedicle measuring less than 1 mm. in external diameter using microsurgical techniques. *Plast Reconstr Surg*. 1967;40:325–329.
8. Kayano S, Hallock GG, Rice DC, et al. Instructional models for dissection techniques of perforator flaps. In: Blondeel P, Morris SF, Hallock GG, Neligan PC eds. *Perforator Flaps: Anatomy, Technique and Clinical Applications*. 2nd ed. Rome: Quality medical publishing, Inc.; 2013;1:97–107.
9. Shurey S, Akelina Y, Legagneux J, et al. The rat model in microsurgery education: classical exercises and new horizons. *Arch Plast Surg*. 2014;41:201–208.
10. Lee S. Historical events on development of experimental microsurgical organ transplantation. *Yonsei Med J*. 2004;45:1115–1120.
11. Siemionow MZ. Microsurgery models. In: Siemionow MZ, ed. *Plastic and Reconstructive Surgery: Experimental Models and Research Designs*. 1st ed. London, United Kingdom: Springer - Verlag; 2015:3–67.
12. Fukui A. Microvascular anastomoses in the rat. In: Tamai S, Usui M, Yoshizu T, eds. *Experimental and Clinical Reconstructive Microsurgery*. 1st ed. Tokyo: Springer-Verlag; 2004:35–43.
13. Hirase Y. Skin and muscle flaps in the rat. In: Tamai S, Usui M, Yoshizu T, eds. *Experimental and Clinical Reconstructive Microsurgery*. 1st ed. Tokyo: Springer-Verlag; 2004:111–114.
14. Morain WD. Historical perspectives. In: Mathes SJ, ed. *Plastic Surgery*. 2nd ed. Philadelphia, Pa.: Saunders; 2006;1:27–34.
15. Santoni-Rugiu P, Sykes PJ. Skin flaps. In: Santoni-Rugiu P, Sykes PJ, eds. *A History of Plastic Surgery*. 1st ed. Leipzig, Germany: Springer; 2007:79–119.
16. Tamai S. The history of microsurgery. In: Tamai S, Usui M, Yoshizu T, eds. *Experimental and Clinical Reconstructive Microsurgery*. 1st ed. Tokyo, Japan: Springer-Verlag; 2003:3–24.
17. Michaels J, 5th, Levine JP, Hazen A, et al. Biologic brachytherapy: ex vivo transduction of microvascular beds for efficient, targeted gene therapy. *Plast Reconstr Surg*. 2006;118:54–65; discussion 66.
18. Lao WW, Wang YL, Ramirez AE, et al. A new rat model for orthotopic abdominal wall allotransplantation. *Plast Reconstr Surg Glob Open*. 2014;2:e136.
19. Valdatta L, Congiu T, Thione A, et al. Do superficial epigastric veins of rats have valves? *Br J Plast Surg*. 2001;54:151–153.
20. Fukui A. Technique of microangiography. In: Tamai S, Usui M, Yoshizu T, eds. *Experimental and Clinical Reconstructive Microsurgery*. 1st ed. Tokyo: Springer-Verlag; 2004:55–56.
21. Sempuku T. Technique for making a Spalteholz cleared specimen. In: Tamai S, Usui M, Yoshizu T, eds. *Experimental and Clinical Reconstructive Microsurgery*. 1st ed. Tokyo: Springer-Verlag; 2004:59–60.
22. Steinke H, Wolff W. A modified Spalteholz technique with preservation of the histology. *Ann Anat*. 2001;183:91–95.
23. Sempuku T. Technique for making a vascular corrosion cast. In: Tamai S, Usui M, Yoshizu T eds. *Experimental and Clinical Reconstructive Microsurgery*. 1st ed. Tokyo: Springer-Verlag; 2004:57–58.
24. Fischer AH, Jacobson KA, Rose J, et al. Hematoxylin and eosin staining of tissue and cell sections. *CSH Protoc*. 2008;2008:pdb.prot4986.
25. Foot NC. The Masson trichrome staining methods in routine laboratory use. *Stain Technol*. 1933;8:101–110.
26. Pusztaszeri MP, Seelentag W, Bosman FT. Immunohistochemical expression of endothelial markers CD31, CD34, von Willebrand factor, and Fli-1 in normal human tissues. *J Histochem Cytochem*. 2006;54:385–395.
27. Raimondo S, Fornaro M, Di Scipio F, et al. Chapter 5: methods and protocols in peripheral nerve regeneration experimental research: part II-morphological techniques. *Int Rev Neurobiol*. 2009;87:81–103.
28. Aharinejad SH, Lametschwandtner A. Identification and interpretation of cast vessel structures. In: Aharinejad SH, Lametschwandtner A, eds. *Microvascular Corrosion Casting in Scanning Electron Microscopy: Techniques and Applications*. 1st ed. New York, N.Y.: Springer-Verlag; 1992:103–115.
29. Sheena Y, Jennison T, Hardwicke JT, et al. Detection of perforators using thermal imaging. *Plast Reconstr Surg*. 2013;132:1603–1610.
30. Gurunluoglu R, Siemionow MZ. The microsurgical groin skin flap in the rat model. In: Siemionow MZ, ed. *Plastic and Reconstructive Surgery: Experimental Models and Research Designs*. 1st ed. London, United Kingdom: Spronger; 2015:53–62.
31. Dunn RM, Mancoll J. Flap models in the rat: a review and reappraisal. *Plast Reconstr Surg*. 1992;90:319–328.
32. Taylor GI, Minabe T. The angiosomes of the mammals and other vertebrates. *Plast Reconstr Surg*. 1992;89:181–215.
33. Taylor GI, Pan WR. The angiosome concept. In: Dodwell P, ed. *The Angiosome Concept and Tissue Transfer*. 1st ed. Saint Louis, Missouri: Quality Medical Publishing, Inc.; 2014;1:354–395.
34. Hallock GG, Rice DC. Physiologic superiority of the anatomic dominant pedicle of the TRAM flap in a rat model. *Plast Reconstr Surg*. 1995;96:111–118.
35. Hallock GG, Rice DC. Cranial epigastric perforator flap: a rat model of a true perforator flap. *Ann Plast Surg*. 2003;50:393–397.
36. Ozkan O, Coşkunfirat OK, Ozgentaş HE, et al. New experimental flap model in the rat: free flow-through epigastric flap. *Microsurgery*. 2004;24:454–458.

11

37. Ozkan O, Koshima I, Gonda K. A supermicrosurgical flap model in the rat: a free true abdominal perforator flap with a short pedicle. *Plast Reconstr Surg.* 2006;117:479–485.

38. Aharinejad SH, Lametschwandtner A. The peripheral sense organs. The integument. In: Aharinejad SH, Lametschwandtner A, eds. *Microvascular Corrosion Casting in Scanning Electron Microscopy: Techniques and Applications.* 1st ed. New York, N.Y.: Springer-Verlag; 1992:354–360.

39. Pearl RM, Johnson D. The vascular supply to the skin: an anatomical and physiological reappraisal—Part II. *Ann Plast Surg.* 1983;11:196–205.

40. Kochi T, Imai Y, Takeda A, et al. Characterization of the arterial anatomy of the murine hindlimb: functional role in the design and understanding of ischemia models. *PLoS One.* 2013;8:e84047.

41. Gagnon A, Blondeell P. Deep and superficial inferior epigastric artery perforator flaps. *Cirugía Plástica Ibero-Latinoamericana.* 2006;32:7–13.

42. Fathi M, Hatamipour E, Fathi HR, et al. The anatomy of superficial inferior epigastric artery flap. *Acta Cir Bras.* 2008;23:429–434.

43. Abu-Hijleh MF, Roshier AL, Al-Shboul Q, et al. The membranous layer of superficial fascia: evidence for its widespread distribution in the body. *Surg Radiol Anat.* 2006;28:606–619.

44. Blondeel PN, Morris NJ, Hallock GG, et al. Vascular territories of the integument. In: Blondeel PN, Morris NJ, Hallock GG, Neligan PC, eds. *Perforator Flaps: Anatomy, Technique and Clinical Implications.* 2nd ed. St. Louis, MO: Quality Medical Publishing, Inc.; 2013;1:26–52.

45. Caggiati A, Phillips M, Lametschwandtner A, et al. Valves in small veins and venules. *Eur J Vasc Endovasc Surg.* 2006;32:447–452.

46. Casal D, Cunha T, Pais D, et al. Systematic review and meta-analysis of unconventional perfusion flaps in clinical practice. *Plast Reconstr Surg.* 2016;138:459–479.

47. Koyama T, Sugihara-Seki M, Sasajima T, et al. Venular valves and retrograde perfusion. In: Swartz HM, Harrison DK, Bruley DF, eds. *Oxygen Transport to Tissue XXXVI.* New York, N.Y.: Springer; 2014;1:317–323.

48. Aharinejad SH, Lametschwandtner A. Microangioarchitecture of selected organ systems: the integument. In: Aharinejad SH, Lametschwandtner A, eds. *Microvascular Corrosion Casting in Scanning Electron Microscopy: Techniques and Applications.* 1st ed. New York, N.Y.: Springer-Verlag; 1992:354–360.

49. Imayama S. Scanning and transmission electron microscope study on the terminal blood vessels of the rat skin. *J Invest Dermatol.* 1981;76:151–157.

50. Walløe L. Arterio-venous anastomoses in the human skin and their role in temperature control. *Temperature (Austin).* 2016;3:92–103.

51. Hirigoyen MB, Rhee JS, Weisz DJ, et al. Reappraisal of the inferior epigastric flap: a new neurovascular flap model in the rat. *Plast Reconstr Surg.* 1996;98:700–705.

52. Millington PF, Wilkinson R. The skin in depth: dermal vasculature. In: Harrison RJ, McMinn RM, eds. *Biologic Structure and Function of the Skin: Skin.* 1st ed. London: Cambridge University Press; 1983;1:69–72.

53. Syed SA, Tasaki Y, Fujii T, et al. A new experimental model: the vascular pedicle cutaneous flap over the dorsal aspect (flank and hip) of the rat. *Br J Plast Surg.* 1992;45:23–25.

54. Ozkan O, Akyürek M, Safak T, et al. A new flap model in rats: iliac osteomusculocutaneous flap. *Ann Plast Surg.* 2001;47:161–167.

55. Nasır S. New modification of the oldest flap in rats to increase antigenicity of transplanted skin: the extended groin flap model. *Plas Reconstr Surg.* 2015;1:227–236.

56. Dunn RM, Huff W, Mancoll J. The rat rectus abdominis myocutaneous flap: a true myocutaneous flap model. *Ann Plast Surg.* 1993;31:352–357.

57. Taylor GI, Watterson PA, Zelt RG. The vascular anatomy of the anterior abdominal wall: the basis for flap design. *Perspect Plast Surg.* 1991;5:1–28.